Indian Journal of Pure & Applied Physics
Vol. 55, July 2017, pp. 478-489

Quantum chemical calculations on the geometrical, conformational, spectroscopic (FTIR, FT-Raman) analysis and NLO activity of milrinone [5-cyano-2-methyl-(3,4'-bipyridin)-6(1h)-one] by using hartree-fock and density functional methods

A Eşme*

Department of Elementary Science Education, Kocaeli University, Kocaeli 41380, Turkey

Received 21 July 2016; revised 18 January 2017; accepted 14 February 2017

The Fourier transform infrared (FTIR) and Fourier transform Raman (FT-Raman) spectra of milrinone [5-Cyano-2-methyl-(3,4'-bipyridin)-6(1H)-one] in solid phase have been recorded and analyzed. Quantum chemical calculations of the optimized molecular structure, energies, molecular surfaces, conformational, nonlinear optical (NLO) properties and vibrational studies of milrinone have been calculated by using hartree-fock (HF) and density functional theory (DFT/B3LYP) with 6-31G(d,p) basis set. Obtained results on the geometric structure are compared with the experimental X-ray diffraction. The calculated highest occupied molecular orbital (HOMO) and the lowest unoccupied molecular orbital (LUMO) energies also confirm that charge transfer occurs within the molecule. Molecular parameters like global hardness (η), global softness (σ) and electronegativity (χ) have been calculated with the results obtained from the HOMO and LUMO molecular orbital energies. Nonlinear optical parameters [mean polarizability (<α>), the anisotropy of the polarizability (<Δα>) and the mean first-order hyperpolarizability (<β>)] of the title compound have been investigated theoretically. A detailed interpretation of the infrared and raman spectra of milrinone have been performed with HF and DFT calculations and the potential energy distribution (PED) obtained from the vibrational energy distribution analysis (VEDA4) program.

Keywords: FTIR, FT-Raman spectra, HF, DFT, Milrinone, Nonlinear optical properties

1 Introduction

2(1H)-Pyridones are also known as 2-pyridinones or 1,2-dihydro-2-oxopyridines, and represent a class of pyridine-containing heterocycles. It is well known that many naturally occurring and synthetic compounds containing a 2-pyridone ring system have a broad spectrum of biological activity[1-3] and have recently received a great attention due to their interesting pharmacological properties. Some of them, such as milrinone and amrinone are members of a new class of nonglycosidic positive inotropic bipyridines which are useful in the treatment of congestive heart[4–7].

In a previous publication, the molecular electrostatic potential (MEPs) and atomic charges of milrinone were investigated on the fully optimized structure using the 3-21G** basis set[8]. The crystal structure of the milrinone [5-Cyano-2-methyl-(3,4'-bipyridin)-6(1H)-one] was synthesized and characterized with X-ray diffraction method by Cody[9]. Literature survey reveals that to the best of our knowledge no *ab initio* (HF) and density functional theory (DFT) spectroscopic and harmonic vibrational frequency calculations of milrinone have been reported up to the present. Hence, the purpose of the present study is to give a complete description of the molecular geometry and the detailed theoretical and experimental investigation on the molecular vibrational spectra of title molecule. Besides, we described and characterized the molecular structure, conformational analysis, the total energy, the frontier molecular orbital energies (E_{HOMO} and E_{LUMO}), molecular electrostatic potential map (MEP) and molecular surfaces, electronegativity (χ), global hardness (η) and global softness (σ) properties, nonlinear optical (NLO) analysis and vibrational frequencies of the investigated molecule in the ground state calculated with HF and DFT/B3LYP levels for the 6-31G(d,p) basis set. The mean first-order hyperpolarizability (<β>) and related properties (dipole moment (μ), the mean polarizability <α> and the anisotropy of the polarizability <Δα>) of title compound were calculated by using the same methods based on the finite-field (FF) approach.

*Corresponding author (E-mail: asliesme@gmail.com)

2 Experimental Details

Milrinone in the solid form was purchased from the Sigma-Aldrich Chemical Company (USA), with a stated purity of greater than 97% and it was used as such to record FTIR and FT-Raman spectra. The Fourier transform infrared (FTIR) spectrum of solid milrinone was recorded using an Agilent Cary 630 FTIR spectrometer with the KBr technique in the region 4000-400 cm^{-1}. The Fourier transform Raman (FT-Raman) spectrum of solid milrinone was measured and recorded in the range of 4000-400 cm^{-1} using 1064 nm line of InGaAs laser as excitation wavelength on a Nicolet NXR FT-Raman spectrophotometer.

3 Computational Details

The quantum mechanical calculations were carried out using Gaussian 09 Rev. 11.4 package program[10] and the obtained results were visualized by Gauss view rev. 5.0.9 software[11]. The molecular structure of the milrinone [5-Cyano-2-methyl-(3,4'-bipyridin)-6(1H)-one] in the ground state was calculated by performing both Hartree–Fock (HF) and the density functional theory (DFT) by a hybrid functional B3LYP (Becke's three parameter hybrid functional using the LYP correlation functional) methods[12,13] at 6-31G(d,p) basis set. The optimized structure parameters (bond lengths, bond angles and dihedral angels), vibrational frequencies, IR and Raman intensities of the milrinone were calculated with HF/6-31G(d,p) and B3LYP/6-31G(d,p) methods and then scaled the frequencies with scaling factors[14,15] 0.8991 and 0.9614, respectively, and these results were compared with the experimental data. Detailed assignments of the computed normal modes were analyzed in terms of the percentage potential energy distribution (PED) contributions by using the vibrational energy distribution analysis (VEDA4) program written by Jamroz[16]. The optimized structure of the title molecule is confirmed to be located at the local true minima on the potential energy surface, as they have not got any imaginary frequency modes.

In the context of the HF theorem, the highest occupied molecular orbital (E_{HOMO}) and the lowest unoccupied molecular orbital (E_{LUMO}) energies are used to approximate the ionization potential (I) and electron affinity (A) given by Koopmans' theorem[17], respectively. The ionization potential ($I = -E_{HOMO}$) is directly proportional to the HOMO energy and the electron affinity ($A = -E_{LUMO}$) is directly proportional to the LUMO energy. Although no formal proof of this theorem exists within density functional theory (DFT), its validity is generally accepted. DFT has been to be successful in providing insights into the chemical reactivity, in terms of molecular parameters such as global hardness (η), global softness (σ) and electronegativity (χ). The global hardness, $\eta = (I - A)/2 = -(E_{HOMO} - E_{LUMO})/2$ is a measure the resistance of an atom to charge transfer[18]. The global softness, $\sigma = 1/\eta = -2/(E_{HOMO} - E_{LUMO})$ describes the capacity of an atom or a group of atoms to receive electrons[18]. Electronegativity, $\chi = (I + A)/2 = -(E_{HOMO} + E_{LUMO})/2$ is a measure of the power of an atom or a group of atoms to attract electrons towards itself[19].

The energy of an uncharged molecule under a weak, general electric field can be expressed by Buckingham type expansion[20-22]:

$$E = E_0 - \mu_i F_i - (1/2)\alpha_{ij} F_i F_j - (1/6)\beta_{ijk} F_i F_j F_k - \ldots (1)$$

where E is the energy of a molecule under the electric field F, E_0 is the unperturbed energy of a free molecule, F_i is the vector component of the electric field in the i direction, and μ_i, α_{ij} and β_{ijk} are the dipole moment, mean polarizability and the mean first-order hyperpolarizability, respectively. Here, each subscript of i, j and k denotes the indices of the Cartesian axes x, y and z. The ground state dipole moment (μ), the mean polarizability <α>, the anisotropy of the polarizability <Δα> and the mean first-order hyperpolarizability (β), using the x, y, z components they are defined as[23,24]:

$$\mu = \left(\mu_x^2 + \mu_y^2 + \mu_z^2\right)^{1/2} \quad \ldots (2)$$

$$\langle\alpha\rangle = \frac{\alpha_{xx} + \alpha_{yy} + \alpha_{zz}}{3} \quad \ldots (3)$$

$$\langle\Delta\alpha\rangle = \left[\frac{(\alpha_{xx} - \alpha_{yy})^2 + (\alpha_{yy} - \alpha_{zz})^2 + (\alpha_{zz} - \alpha_{xx})^2 + 6(\alpha_{xy}^2 + \alpha_{xz}^2 + \alpha_{yz}^2)}{2}\right]^{1/2} \quad \ldots (4)$$

$$\beta = \sqrt{(\beta_{xxx} + \beta_{xyy} + \beta_{xzz})^2 + (\beta_{yyy} + \beta_{yzz} + \beta_{yxx})^2 + (\beta_{zzz} + \beta_{zxx} + \beta_{zyy})^2} \quad \ldots (5)$$

The mean polarizability and the mean first-order hyperpolarizability tensors α_{xx}, α_{xy}, α_{yy}, α_{xz}, α_{yz}, α_{zz} and β_{xxx}, β_{xxy}, β_{xyy}, β_{yyy}, β_{xxz}, β_{xyz}, β_{yyz}, β_{xzz}, β_{yzz}, β_{zzz} can be obtained by frequency job output file[10] of GAUSSIAN-09W. Since the values of the mean polarizabilities (α) and first-order hyperpolarizability (β) of GAUSSIAN-09W output are reported in atomic units (a.u.), the calculated values have been converted into electrostatic units[25] (esu) (α: 1 a.u. = 0.1482×10^{-24} esu; β:1 a.u. = 8.6393×10^{-33} esu).

4 Results and Discussion

4.1 Geometric structure

The crystal structure of milrinone [5-Cyano-2-methyl-(3,4'-bipyridin)-6(1H)-one] [$C_{12}H_9N_3O$] was taken from Cambridge Crystallographic Data Center (CCDC 1156532). The crystal structure parameters[9] of milrinone are a =3.8380(3) Å, b =13.1010(12) Å, c =8.0980(8) Å, β=96.010(4)^0 and V=404.94(6) Å^3. It was synthesized by Cody[9] and the optimized molecular structure with the atom numbering scheme obtained from B3LYP/6-31G(d,p) level is shown in Fig. 1. Obtained optimized structure parameters (bond lengths, bond angles and dihedral angles) for milrinone calculated with *ab* initio HF and B3LYP methods using 6-31G(d,p) basis set are listed in the Table 1 and compared with experimental parameters available from X-ray diffraction data[9]. The investigated compound milrinone has similar pyridine rings same as amrinone except for substituent groups attached to the pyridine ring. Therefore we have compared the calculated structural parameters of the milrinone and amrinone with experimentally available values from the X-ray study[9] and have presented in Table 1.

From the Table 1, the calculated optimized structure parameters obtained from HF and B3LYP levels are in very good agreement with the experimental values. As seen from Table 1, while the optimized C-C bonds of the rings lie in the range of 1.351–1.458 Å and 1.339–1.473 Å for HF/6-31G(d,p) and 1.376–1.461 Å and 1.369–1.469 Å for B3LYP/6-31G(d,p) levels, the experimental C-C values fall in the range of 1.374–1.437 Å and 1.346–1.421 Å for milrinone and amrinone, respectively.

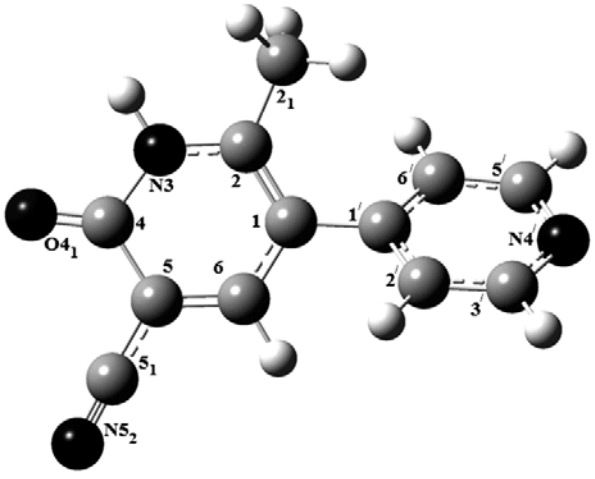

Fig. 1 — Optimized molecular structure with atomic numbering scheme obtained using B3LYP/6-31G(d,p) method of milrinone

The bond lengths and bond angles of the cyano group (C≡N) confirm linearity which is a quite commonly feature observed in carbonitrile compounds[26]. Sert *et al.*[27] calculated this bond length as 1.155 Å for B3LYP/6-311++G(d,p) and 1.130 Å for HF/6-311++G(d,p).

In milrinone and amrinone molecules, the experimental $C5_1{\equiv}N5_2$ and C5-N5 bond lengths[9] were observed as 1.140 and 1.368 Å, respectively. In our calculations, at the B3LYP/6-31G(d,p) and HF/6-31G(d,p) methods, the cyano group bond length for milrinone is 1.163 and 1.136 Å, whereas the C5-N5 bond length for amrinone is 1.374 and 1.378 Å, respectively. Further the result of our calculations showed that ($C5_1{\equiv}N5_2$) bond shows typical triple bond characteristics, whereas (C5-N5) bond shows single bond characteristics. The bond angle of the cyano group ($C5\text{-}C5_1\text{-}N5_2$) was 177.92° at HF/6-31G(d,p) and 178.47° at B3LYP/6-31G(d,p).

The $C4{=}O4_1$ bond length[9] was found at 1.240 Å for milrinone and 1.263 Å for amrinone and this bond was computed at 1.197 and 1.221 Å for milrinone and 1.207 and 1.234 Å for amrinone at HF and B3LYP levels with 6-31G(d,p) basis set, respectively. The $C4{=}O4_1$ bond length is consistent with the C=O double bonding. This bond distance is comparable with those of compounds previously reported as 2-pyridone[28,29].

To make comparison with experimental results, we present linear correlation coefficients (R^2) for linear regression analysis of theoretical and experimental bond lengths and angles. These coefficients can be seen in the last line of Table 1. Correlation graphic for the calculated at HF/6-31G(d,p) and B3LYP/6-31G(d,p) levels and experimental bond lengths and bond angles are shown in Fig. 2. The bond lengths calculated by using the HF and B3LYP methods with 6-31G(d,p) basis set for milrinone and amrinone correlate fairly with experimental data (R^2 is 0.985 (HF method) and 0.987 (B3LYP method) for milrinone and 0.914 (HF method) and 0.976 (B3LYP method) for amrinone, respectively). For bond angles, R^2 is 0.986 (HF method) and 0.986 (B3LYP method) for milrinone and 0.893 (HF method) and 0.899 (B3LYP method) for amrinone, respectively. It is evident that both methods give the most satisfactory correlations between experimental and calculated bond lengths and angles.

Visualizing and describing the relationship between potential energy and molecular geometry is called a

Table 1 — Bond lengths, bond angles and dihedral angles calculated for milrinone and amrinone using HF/6-31G(d,p) and B3LYP/6-31G(d,p) methods compared with experimental data[9]

Parameters	Experimental[a] (Ref.[9])	Experimental[b] (Ref.[9])	HF[a]	B3LYP[a]	HF[b]	B3LYP[b]	Parameters	Experimental[a] (Ref.[9])	Experimental[b] (Ref.[9])	HF[a]	B3LYP[a]	HF[b]	B3LYP[b]
		Bond lengths (Å)						Bond angles (°)					
C1-C1′	1.484	1.477	1.492	1.485	1.485	1.479	C1′-C1-C2	123.55	121.69	124.12	123.53	121.31	120.66
C1-C2	1.386	1.346	1.358	1.386	1.339	1.369	C1-C2-N3	119.02	122.02	119.44	118.64	120.43	119.98
C1-C6	1.403	1.417	1.433	1.425	1.447	1.435	C2-N3-C4	126.61	123.17	127.37	128.06	125.44	125.80
C2-N3	1.359	1.357	1.362	1.365	1.373	1.373	N3-C4-$O4_1$	120.97	120.20	120.69	120.23	122.17	122.10
C4-C5	1.437	1.421	1.458	1.461	1.473	1.469	N3-C4-C5	113.88	116.98	112.73	112.12	114.66	114.19
C4-N3	1.372	1.354	1.384	1.412	1.361	1.386	C1-C1′-C6′	122.55	121.08	122.09	122.58	121.78	121.95
C4-$O4_1$	1.240	1.263	1.197	1.221	1.207	1.234	C1′-C6′-C5′	118.88	120.58	119.03	119.33	119.14	119.54
C5-C6	1.374	1.389	1.351	1.376	1.345	1.373	C6′-C5′-N4′	124.68	123.65	123.72	123.98	123.89	124.11
C1′-C2′	1.390	1.380	1.390	1.403	1.391	1.404	C5′-N4′-C3′	115.92	115.83	117.38	116.63	117.07	116.30
C1′-C6′	1.392	1.411	1.389	1.403	1.391	1.404	N4′-C3′-C2′	123.78	124.04	123.70	123.95	123.92	124.16
C2′-C3′	1.384	1.390	1.384	1.394	1.383	1.393	C2′-C1′-C1	120.34	123.42	120.74	120.65	121.35	121.64
C3′-N4′	1.336	1.337	1.320	1.339	1.321	1.339	C6-C1-C1′	118.83	120.55	118.83	119.09	120.87	121.30
C5′-C6′	1.380	1.373	1.385	1.395	1.384	1.393	C4-C5-N5	-	116.40	-	-	114.20	113.49
C5′-N4′	1.338	1.349	1.320	1.338	1.320	1.340	C5-$C5_1$-$N5_2$	178.55	-	177.92	178.47	-	-
C5-N5	-	1.368	-	-	1.378	1.374	C1-C2-$C2_1$	126.11	-	126.15	126.10	-	-
C2-$C2_1$	1.499	-	1.503	1.504	-	-	C4-C5-$C5_1$	118.00	-	118.49	118.19	-	-
C5-$C5_1$	1.435	-	1.438	1.427	-	-	N3-C2-$C2_1$	114.85	-	114.40	115.24	-	-
$C5_1$-$N5_2$	1.140	-	1.136	1.163	-	-	C6-C5-$C5_1$	121.29	-	121.05	121.19	-	
Corr. coefficient			0.985	0.987	0.914	0.976				0.986	0.986	0.893	0.899
							Dihedral angles (°)						
C1′-C1-C6-C5	-177.58	175.75	-179.49	-179.67	178.90	178.85	C6-C1-C1′-C6′	134.33	170.60	119.17	129.79	139.03	146.50
C2-N3-C4-$O4_1$	-177.15	178.87	-179.77	-179.75	-178.42	-178.42	C1-C1′-C6′-C5′	-176.88	179.19	-178.71	-178.80	179.03	179.18
C2-C1-C1′-C2′	137.83	167.64	120.83	130.97	137.31	145.16	C1-C1′-C2′-C3′	175.97	-179.95	178.46	178.56	-179.27	-179.57
C6-C1-C1′-C2′	-42.56	-8.20	-58.78	-48.13	-41.27	-33.63	C1′-C6′-C5′-N4′	0.77	1.47	0.48	0.52	0.54	0.70
C6′-C5′-N4′-C3′	-0.59	-0.14	0.06	0.10	-0.09	-0.23	C5-C6-C1-C1′	-177.58	175.75	-179.49	-179.67	178.90	178.85
C1′-C1-C2-$C2_1$	-5.65	-	-1.52	-1.81	-	-	$O4_1$-C4-C5-N5	-	-2.60	-	-	-3.35	-3.05
N3-C4-C5-$C5_1$	177.16	-	179.73	179.68	-	-	N3-C4-C5-N5	-	177.50	-	-	177.54	177.81
$O4_1$-C4-C5-$C5_1$	-3.16	-	-0.06	-0.01	-	-	C1-C6-C5-N5	-	-176.50	-	-	-177.79	-178.00
$C2_1$-C2-N3-C4	-177.23	-	-178.85	-178.30	-	-							

*Experimental geometrical parameters (bond lengths, bond angles and dihedral angles) of [a]Milrinone, [b]Amrinone molecules

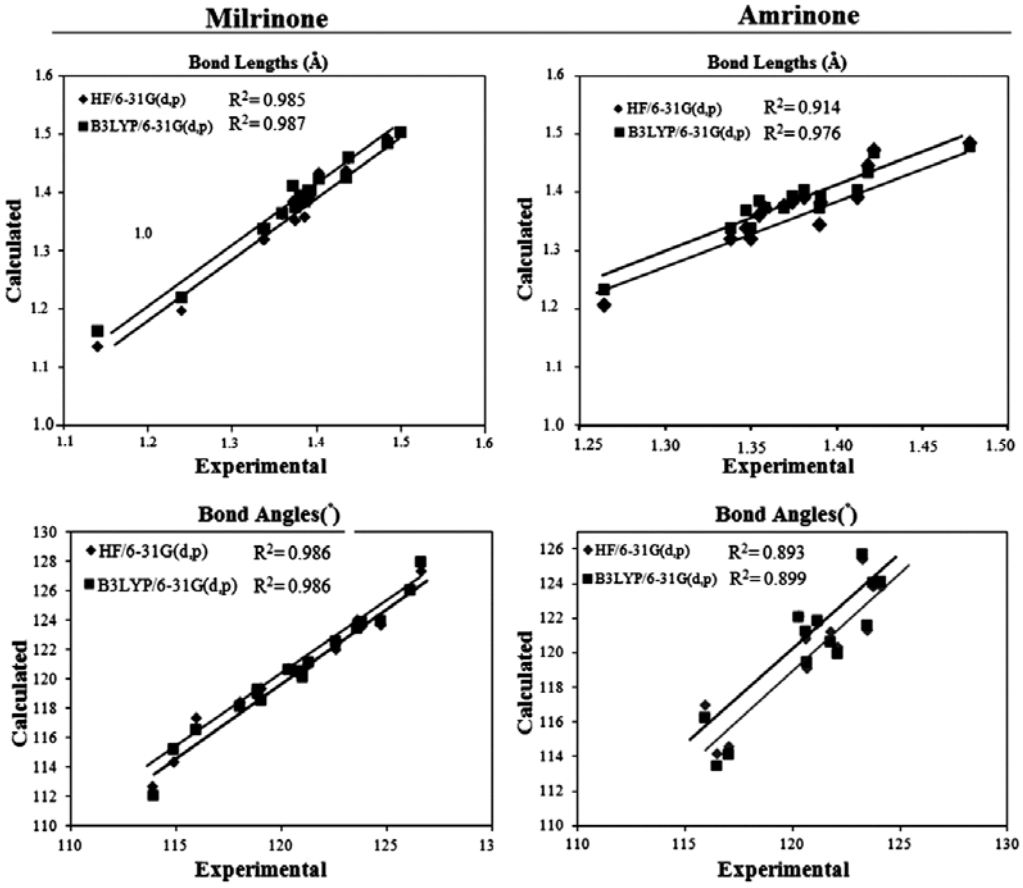

Fig. 2 — Linear relationships of experimental[9] and calculated (with 6-31G(d,p) level) molecular bond lengths and molecular bond angles of milrinone and amrinone

potential energy surface (PES) that is an important to reveal all possible conformations of the title molecule. A detailed PES scan on dihedral angle C2-C1-C1′-C2′ between the two pyridine rings has been performed at the HF/6-31G(d,p) method to determine the most stable conformers of milrinone [5-Cyano-2-methyl-(3,4'-bipyridin)-6(1H)-one]. According to X-ray study[9], dihedral angle of C2-C1-C1′-C2′ between the two pyridine rings is 137.83°, whereas it has been calculated at 130.97° for B3LYP and 120.83° for HF methods, leading to an expected bent conformation of the molecule. The C2-C1-C1′-C2′ dihedral angle values predicted theoretically were (120.83° for HF and 130. 97° for B3LYP) shorter by 17° and 6.86° when compared with X-ray data (137.83º), respectively. For conformational analysis of the milrinone molecule, starting from the optimized molecular structure given in Fig. 1, the C2-C1-C1′-C2′ dihedral angle was increased by 10° steps from 0° to 360°, while all of the other geometrical parameters have been simultaneously relaxed. PES scan for the selected dihedral angle is depicted in Fig. 3. As clearly seen from the curve in the Fig. 3, global minimum point (i.e., the most stable structure) is calculated at 297° with the -697.898869 Hartree energy value. The energy of local minimum point calculated at 237° was predicted as -697.898867 Hartree.

4.2 Vibrational analysis

The entire set of quantum chemical calculations was performed using the Hartree–Fock (HF) and density functional theory (DFT) calculations with B3LYP level using 6-31G(d,p) as a basis set using Gaussian 09 Rev. A 11.4 package program[10] program package. The observed (FTIR and FT-Raman) and calculated IR intensities, Raman activities and assigned wavenumbers of the selected intense vibrational modes by using HF/6-31G(d,p) and B3LYP6-31G(d,p) levels along with their PED values of the milrinone are given in Table 2. The obtained

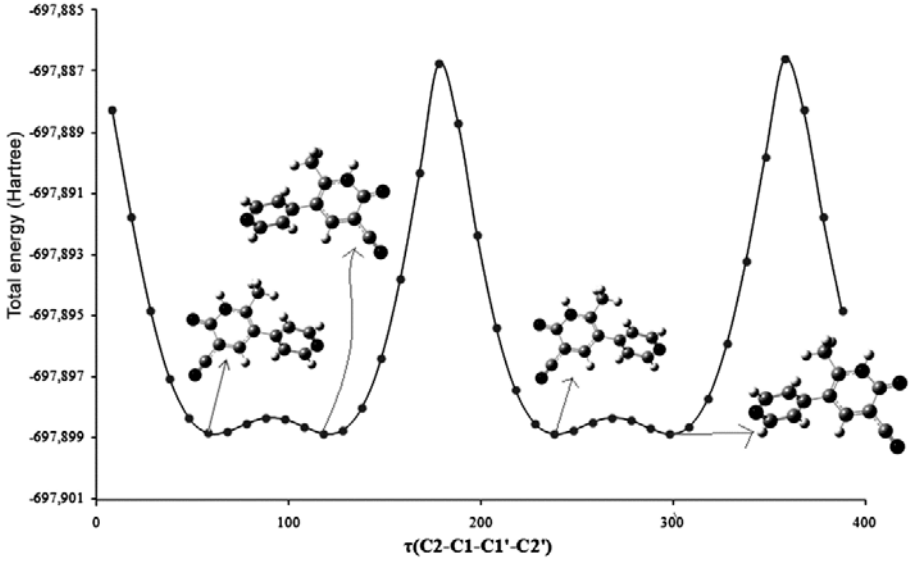

Fig. 3 — One-dimensional potential energy surface (PES) scan of the milrinone using HF level with 6-31G(d,p) basis set

harmonic frequencies were scaled by 0.8991 in case[14] of HF/6-31G(d,p) and 0.9614 in case[15] of B3LYP/6-31G(d,p) methods to obtain a better agreement between the theory and the experiment. The experimental and theoretical FTIR and FT-Raman spectra are shown in Figs 4 and 5, respectively.

4.2.1 C≡N, C=N and C-N vibrations

The geometry of the cyano group (C≡N) is affected insignificantly by a new substituent on the phenyl ring. Hence the vibrational wavenumber on the cyano group remains almost unchanged from the benzonitro molecule. For the aromatic compound which bears a C≡N group attached to the ring, a band of good intensity has been absorbed in the region 2260–2221 cm^{-1} and it is being attributed to C≡N stretching[30]. Electron-withdrawing groups, such as Cl, F, Br, $–NO_2$, –OH or $–CF_3$, decrease the IR band intensity and increase the wavenumber value to the higher limit of the characteristic spectral region, whereas electron donating groups, such as $–NH_2$ and $–CH_3$, increase IR intensity and decrease wavenumber value[31]. In our present work, theoretically computed value (ν9) is assigned to the stretching of C≡N group which is contributing to 89% of PED, and it is in a good agreement with our experimental spectrum observed as the medium peak in FTIR and the very strong band in FT-Raman spectrum (Table 2) at both 2222 cm^{-1}. The vibrational mode (ν9), which is calculated at 2346 and 2258 cm^{-1} for HF and B3LYP levels with 6-31G(d,p) basis set is assigned to the in-plane stretching vibration of C≡N group. In-plane and out-of-plane bending modes of C≡N group appear with weak IR intensity and strong raman activity. In plane bending modes of C≡N group are calculated at 459, 444 cm^{-1} and 444, 433 cm^{-1} by using HF and B3LYP levels, respectively, and observed at 462, 414 cm^{-1} in FTIR spectra and at 459, 417 cm^{-1} in FT-Raman spectra. In out-of-plane bending vibration of C≡N group is calculated at 520 and 503 cm^{-1} by using HF and B3LYP levels, respectively. The out-of-plane bending vibration of C≡N group is observed at 529 cm^{-1} in FTIR spectrum and at 528 cm^{-1} in FT-Raman spectrum.

The identification of C=N and C-N vibrations are very difficult task because mixing of several modes is possible in this region. The pyridine ring C=N stretching vibration modes[32] appear strongly in the region 1600–1500 cm^{-1}. Pyridine C=N stretching vibration was observed to be 1573 and 1568 cm^{-1} in FTIR and FT-Raman spectra experimentally, while that has been calculated at 1586 and 1544 cm^{-1} for HF/6-31G(d,p) and B3LYP/6-31G(d,p) methods, respectively. The C-N stretching vibration modes[33] of pyridine ring are always coupled with other vibration and usually appear in the region 1380–1265 cm^{-1}. The calculated C-N stretching vibrations fall in the region 1255–1019 cm^{-1} for HF method and 1259–1008 cm^{-1} for B3LYP method. The ring C-N stretching vibrational modes were assigned at 1219, 1133, 1088 and 1014 cm^{-1} in FTIR and 1219, 1134, 1080 and 991 cm^{-1} in Raman spectra, respectively.

Table 2 — Comparison of the observed (FTIR and FT-Raman) and calculated vibrational wavenumbers, IR intensities and Raman activities and potential energy distribution (PED) using HF/6-31G(d,p) and B3LYP/6-31G(d,p) of milrinone

		Experimental		Theoretical							
		FTIR	FT-Raman	HF/6-31G(d,p)				B3LYP/6-31G(d,p)			
ν	Assignments (%PED[a])			A^b	B^c	IR intensity	Raman activity	A^b	B^c	IR intensity	Raman activity
1	ν(NH) (100)	3451	3452	3852	3463	101	74	3593	3454	67	106
2	ν(CH) (84)	3049	3056	3374	3034	4	188	3206	3083	2	147
3	ν(CH) (92)	3019	3032	3372	3032	8	43	3205	3081	9	22
4	ν(CH) (91)	2993	2999	3370	3030	17	31	3201	3077	8	50
5	$\nu(CH_3)$ (89)	2967	2972	3336	2999	6	51	3174	3052	2	42
6	$\nu_{as}(CH)$ (91)	2919	2929	3346	3008	22	68	3167	3045	26	156
7	$\nu_{as}(CH_3)$ (89)	2904	2900	3254	2926	11	99	3104	2984	9	104
8	$\nu(CH_3)$ (100)	2859	2857	3195	2873	18	193	3047	2929	13	238
9	ν(C≡N) (89), ν(CC) (11)	2222	2222	2609	2346	64	376	2349	2258	26	557
10	ν(C=O) (77), σ(CNC) (11)	1767	1762	1969	1770	920	22	1801	1731	594	26
11	ν(CC) (57), σ(HCC) (13)	1666	1645	1830	1645	96	64	1652	1588	28	150
12	ν(CC) (29)	1595	1606	1809	1627	109	38	1647	1583	118	173
13	ν(CC) (21), ν(NC) (20)	1573	1568	1764	1586	143	88	1606	1544	92	89
14	ν(CC) (18), ν(NC) (12), δ(HNC) (10)	1546	1539	1748	1572	166	158	1586	1525	93	174
15	δ(HCC) (23), δ(HNC) (40)	1487	1485	1677	1508	15	10	1538	1479	12	22
16	$\sigma(CH_3)$ (33), δ(HNC) (16), ν(NC) (13)	1435	1437	1635	1471	39	39	1508	1450	7	25
17	$\sigma(CH_3)$ (77)	1416	1429	1617	1454	5	14	1500	1442	9	16
18	$\sigma(CH_3)$ (33), δ(HNC) (10), ν(NC) (10)	1387	1396	1601	1440	28	41	1478	1421	32	72
19	ν(CC) (27), δ(HCN) (48)	1372	1375	1566	1408	30	3	1452	1396	24	9
20	$\beta(CH_3)$ (90)	1349	1346	1555	1398	1	16	1428	1373	1	32
21	δ(HCC) (11), ν(CC) (39)	1320	1327	1520	1367	19	94	1406	1352	5	145
22	δ(HCC) (38), δ(HCN) (30)	1279	1282	1471	1323	5	6	1361	1309	2	11
23	δ(HCC) (15), δ(HNC) (28), ν(CC) (12)	1238	1246	1427	1283	54	24	1323	1272	35	26
24	ν(NC) (19), ν(CC) (21), σ(CCC) (10)	1219	1219	1396	1255	53	12	1310	1259	34	46
25	δ(HCC) (22), δ(HNC) (41)	1178	1180	1346	1210	7	8	1253	1205	4	10
26	ν(CC) (55)	1133	1134	1255	1128	35	53	1189	1143	18	7
27	ν(CC) (17), ν(NC) (34)	1088	1080	1230	1106	15	31	1128	1085	31	24
28	β(CCN) (38), δ(HCC) (18)	1074	1057	1183	1064	0	2	1097	1055	0	0
29	τ(HCCN) (54), $\sigma(CH_3)$ (16)	1036	1040	1163	1046	3	3	1062	1021	6	4
30	ν(NC) (10), τ(HCCN) (10)	1014	991	1133	1019	6	13	1048	1008	19	0
31	γ(HCCN) (33)	988	960	1100	989	2	6	1015	976	3	7
32	β(CCN) (34), β(CNC) (13), ν(NC) (36)	876	877	1092	982	5	39	1011	972	46	0
33	ω(HCCN) (77), τ(HCNC) (21)	831	839	940	845	27	1	892	858	0	12
34	γ(ONCC) (72), γ(HNCC) (12)	801	783	880	791	67	5	783	753	41	2
35	σ(CCC) (18), ν(CC) (43), ν(NC) (10)	731	733	786	707	4	2	735	707	1	29
36	γ(HNCC) (56), γ(CNCC) (12)	686	679	758	682	22	2	721	693	33	3
37	δ(CCC) (16), β(CCN) (21), β(CNC) (13)	-	-	737	663	24	2	688	661	7	5
38	ν(CC) (12), β(CNC) (14), σ(NCC) (19)	652	652	732	658	8	2	685	659	6	2
39	γ(CCCC) (14)	-	-	716	644	15	9	660	635	6	4
40	σ(CCC) (14), σ(OCN) (11)	-	629	706	635	10	1	651	626	7	2
41	σ(CNC) (13)	589	584	639	575	28	1	590	567	20	2
42	γ(CCCC) (28)	-	559	595	535	19	3	542	521	10	2
43	γ(CCCC) (25), γ(ONCC) (12), γ(NCCC) (46)	529	528	578	520	15	10	523	503	9	6
44	β(NCC) (18), β(CCC) (11), γ(CNCC) (15)	462	459	511	459	3	2	462	444	2	5
45	σ(NCC) (13), β(NCC) (13)	414	417	494	444	12	1	450	433	10	2

ν, stretching vibrations; β, in-plane bending vibrations; γ, out-of-plane bending vibrations; ω , wagging; τ, twisting; σ, scissoring; δ, rocking; s, simetric; as, antisimetric.

[a] Potential Energy Distribution (PED) less then 10% are not shown.

[b] Unscaled wavenumbers.

[c] Scaled wavenumbers.

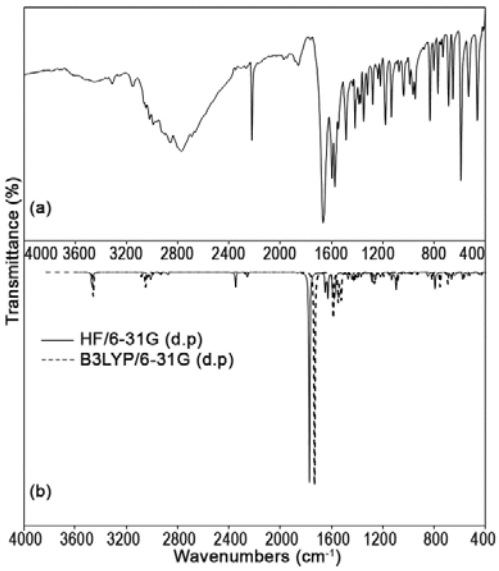

Fig. 4 — (a) Experimental FTIR spectrum in the wavenumber range 4000–400 cm^{-1} and (b) simulated FTIR spectrum computed at HF and B3LYP levels with 6-31G(d,p) basis set of milrinone

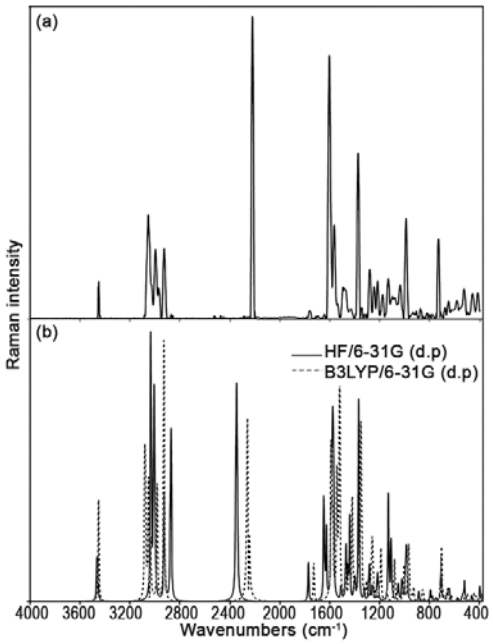

Fig. 5 — (a) Observed FT-Raman spectrum of milrinone in the wavenumber range 4000–400 cm^{-1} and (b) the simulated Raman spectrum computed at HF and B3LYP levels with 6-31G(d,p) basis set of the milrinone

4.2.2 Methyl group vibrations

The vibrational peaks due to the asymmetric and symmetric methyl stretching modes have been usually expected in the range 2905-3000 cm^{-1} and 2860-2870 cm^{-1}, respectively[31,34]. While the asymmetric stretching vibration of the methyl group has been calculated at 2926 cm^{-1} using HF and 2984 cm^{-1} using B3LYP levels, the symmetric methyl stretching vibrations for milrinone have been calculated at 2999, 2873 cm^{-1} and 3052, 2929 cm^{-1} by using HF and B3LYP levels with 6-31G(d,p) basis set, respectively. These peaks have been observed at the region of 2967-2859 cm^{-1} in FTIR and 2972-2857 cm^{-1} in FT-Raman, as consistent with literature[35-37]. The methyl in-plane bending vibration has been observed at 1349 cm^{-1} in the FTIR and 1346 cm^{-1} in the FT-Raman bands. The vibrational mode (ν20), which is calculated at 1398 and 1373 cm^{-1} for HF and B3LYP levels with the 90% contribution of PED are assigned to the in-plane bending vibrations of the methyl group. Our in-plane bending vibration of the methyl group is in accordance with literature data[38].

4.2.3 C-H vibrations

The aromatic structure shows the presence of C-H stretching vibrations in the region 2900–3150 cm^{-1}, which is the characteristic region for the identification of the C-H stretching vibrations. In this region, the bands are not affected appreciably by the nature of substituents[39]. In the FTIR and FT-Raman spectra of milrinone, the bands observed at 3049, 3019, 2993 and 2919 cm^{-1} and 3056, 3032, 2999 and 2929 cm^{-1} are assigned to C-H stretching vibrations of aromatic ring, respectively. The theoretically scaled vibrations by HF/6-31G(d,p) and B3LYP/6-31G(d,p) methods at 3034, 3032, 3030 and 3008 cm^{-1} and 3083, 3081, 3077 and 3045 cm^{-1}, respectively, are assigned to C-H stretching vibrations. As evidenced from PED contributions in Table 2, these modes are pure stretching vibrations almost contributing to the range 84–92%.

The C–H in-plane bending vibrations and the C-H out-of-plane bending vibrations normally appear in the range 1100–1500 cm^{-1} and 750–1000 cm^{-1} frequency regions, respectively[40,41]. In this study, the C–H in-plane bending vibrations are assigned to 1487, 1320, 1279, 1238, 1178, 1074 cm^{-1} in FT-IR and 1485, 1327, 1282, 1246, 1180, 1057 cm^{-1} in FT-Raman spectra. In plane ones are calculated at 1508, 1367, 1323, 1283, 1210, 1064 cm^{-1} and 1479, 1352, 1309, 1272, 1205, 1055 cm^{-1} by using HF and B3LYP methods, respectively. The band observed at 831 and 839 cm^{-1} in FTIR and FT-Raman spectra, respectively, is assigned to C-H out-of-plane bending vibration for the title compound. The HF and DFT calculations give the modes at 845 and 858 cm^{-1}, respectively.

4.2.4 C=O vibrations

The carbonyl group is present in a large number of different classes of compounds, for which a strong band observed due to the C=O stretching vibration[32] that is in the region of 1850–1550 cm^{-1}. Band observed at 1767 and 1762 cm^{-1} in FTIR and FT-Raman spectra has been assigned mainly to C=O stretching band on the basis of calculated PED (77%), respectively. This characteristic C=O band is calculated at 1770 and 1731 cm^{-1} for HF and B3LYP levels with 6-31G(d,p) basis set, respectively.

4.2.5 N-H vibrations

In heterocyclic molecules, the N-H stretching vibrations[42] have been observed at the range of 3500–3000 cm^{-1}. In the FTIR and FT-Raman spectra of milrinone, respectively, the band observed at 3451 and 3452 cm^{-1} is assigned to N-H stretching vibration of aromatic ring. In our calculations, this peak is calculated at 3463 and 3454 cm^{-1} for HF and B3LYP levels, respectively. This peak is a pure vibration mode which originated from N-H stretching vibration with 100% contribution of PED. As seen from PED analysis in Table 2, the N–H in-plane bending (δHNC) vibrations contribute to the calculated four frequencies at 1572, 1471, 1440 and 1283 cm^{-1} (HF level) and 1525, 1450, 1421 and 1272 cm^{-1} (B3LYP level). These frequencies were assigned to the bands at 1546, 1435, 1387 and 1238 cm^{-1} in FTIR and 1539, 1437, 1396 and 1246 cm^{-1} in FT-Raman. As evidenced from PED contributions in Table 2, these modes are contributed to the range 10–28%. The scaled vibrational frequencies computed by HF/6-31G(d,p) and B3LYP/6-31G(d,p) methods at 791, 682 cm^{-1} and 753, 693 cm^{-1}, respectively, were assigned to the N–H out of bending (γHNCC) vibrations which show good correlation with recorded spectrum at 801, 686 cm^{-1} in FTIR and 783, 679 cm^{-1} in FT-Raman spectra.

4.3 Frontier molecular orbitals (FMOs)

The frontier molecular orbitals (FMOs) called the highest occupied molecular orbital (HOMO) and the lowest unoccupied molecular orbital (LUMO) play an important role in the electric and optical properties, as well as chemical reactions for quantum chemistry[43]. The HOMO (ability to donate an electron) implies the outermost orbital filled by electrons and is directly related to the ionization potential while the LUMO (ability to obtain an electron) can be thought as the first empty innermost orbital unfilled by electron and is directly related to the electron affinity. The HOMO-LUMO 3D orbital pictures computed at the B3LYP/6-31G(d,p) level for the milrinone are given in Fig. 6(a, b). As seen from Fig. 6(a, b) the HOMO of milrinone is largely delocalized almost over the whole molecular moiety but the LUMO of this compound is mainly delocalized on the whole of structure except pyridine ring.

The calculated values for the E_{HOMO} and E_{LUMO} and the frontier molecular orbital energy gap ($\Delta E_{LUMO-HOMO}$) with HF/6-31G(d,p) and B3LYP/6-31G(d,p) levels are given in Table 3. The energy difference between LUMO and HOMO which is called as energy gap helps characterize the chemical reactivity and kinetic stability of the molecule. A soft molecule has a small HOMO-LUMO gap and is more reactive and less stable than hard one with large HOMO-LUMO gap[44]. The calculated values of the energy gap

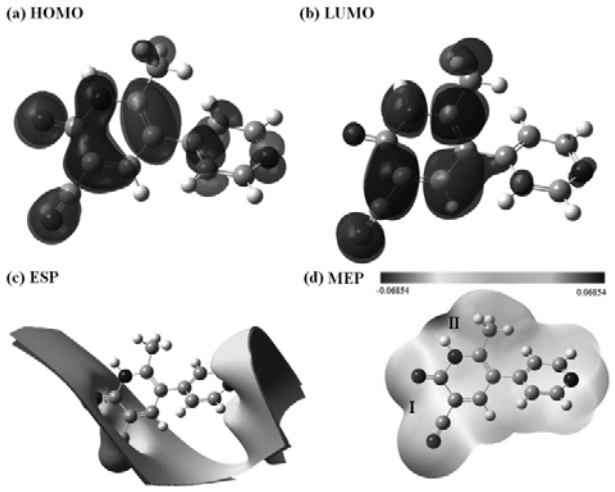

Fig. 6 — The 3D orbital pictures of (a) HOMO, (b) LUMO, (c) electrostatic potential (ESP) and (d) molecular electrostatic potential (MEP) calculated at the B3LYP/6-31G(d,p) level for the milrinone

Table 3 — Total energy, E_{HOMO}, E_{LUMO}, $\Delta E_{LUMO-HOMO}$, ionization potential (I), electron affinity (A), global hardness (η), global softness (σ) and electronegativity (χ) values of milrinone

	HF/6-31G(d,p)	B3LYP/6-31G(d,p)
Total energy (a.u.)	-697.8989	-702.1857
E_{HOMO} (eV)	-8.9376	-6.4635
E_{LUMO} (eV)	1.5483	-2.2493
$\Delta E_{LUMO-HOMO}$	10.4859	4.2142
I	8.9376	6.4635
A	-1.5483	2.2493
η (eV)	5.2430	2.1071
σ (eV^{-1})	0.1907	0.4746
χ (eV)	3.6947	4.3564

for milrinone are 10.4859 and 4.2142 eV for HF and B3LYP levels, respectively. The lower values of HOMO-LUMO energy gap explain the eventual charge transfer interactions taking place within the milrinone molecule. Thus, it is more polarizable, more reactive and less stable. It is also termed as soft molecule.

Development of new chemical reactivity descriptors has gained significant momentum due to their applications in various areas of chemistry, biology, rational drug design and computer-aided toxicity prediction[45]. Global hardness (η), global softness (σ) and electronegativity (χ) are global reactivity descriptors, highly successful in predicting global chemical reactivity trends. By using the above equations, the global chemical reactivity descriptors of molecule such as the global hardness (η), global softness (σ) and electronegativity (χ) have been calculated at HF/6-31G(d,p) and B3LYP/6-31G(d,p) levels for milrinone and their values are shown in Table 3. The global hardness (η) and global softness (σ) correspond to the gap between the E_{HOMO} and E_{LUMO} orbital energies and have been associated with the stability of chemical system. The electronegativity is predicted to be 3.6947 and 4.3564 eV, while the global hardness is predicted to be 5.2430 and 2.1071 eV for the HF and B3LYP levels, respectively.

4.4 Molecular electrostatic surfaces

Molecular electrostatic potential (MEP), $V(r)$, at a given point $r(x, y, z)$ in the vicinity of a molecule, is defined in terms of the interaction energy between the electrical charge generated from the molecule's electrons and nuclei and a positive test charge (a proton) located at r. For the system studied the $V(r)$ values were calculated as described previously using the equation[46]:

$$V(r) = \sum_{A} \frac{Z_A}{(R_A - r)} - \int \frac{\rho(r')}{(r' - r)} dr' \quad \ldots (6)$$

where Z_A is the charge of nucleus A, located at R_A, $\rho(r')$ is the electronic density function of the molecule, and r' is the dummy integration variable. The molecular electrostatic potential is related to the electronic density and is a very useful descriptor in determining sites for electrophilic attack and nucleophilic reactivity as well as hydrogen-bonding interactions[47,48].

In the present study, the 3D plots of electrostatic potential (ESP) and molecular electrostatic potential (MEP) surfaces of milrinone at B3LYP/6-31G(d,p) level are illustrated in Fig. 6(c, d). The MEP maps of milrinone are shown in Fig. 6(d), whereas electrophilic attack is presented by negative (red) regions, nucleophilic reactivity is shown by positive (blue) regions of MEP map of milrinone. As seen from the Fig. 6(d), the negative electrostatic potential regions (*I*) are mainly localized on 3-cyano (C≡N) and carbonyl (C=O) group, showing the most favorable site for electrophilic attack. On the other hand, when focused on positive regions of the electrostatic potential (II), we found that the hydrogen atoms of pyridine ring and N-H atom are surrounded by blue color, indicating that these sites are probably involved in nucleophillic processes. It can be seen from the ESP figure (Fig. 6(c)), that the negative ESP is localized more over the 3-cyano (C≡N), carbonyl (C=O) group and N atom of pyridine ring and is reflected as a yellowish blob.

4.5 Nonlinear optical (NLO) effects

In the present study, the dipole moment (μ), the mean polarizability (<α>), the anisotropy of the polarizability (<Δα>) and the mean first-order hyperpolarizability (<β>) of milrinone have been calculated at HF and DFT/B3LYP methods with the 6-31G(d,p) basis set and given in Table 4. It is known that the significance of the polarizability and the mean first-order hyperpolarizability of molecular system is dependent on the efficiency of electronic communication between acceptor and the donor groups as that will be the key to intra molecular charge transfer[49–52]. It is well known that the higher values of dipole moment, molecular polarizability and hyperpolarizability are important for more active NLO properties. According to the present calculations in Table 4, the calculated dipole moments and the mean first-order hyperpolarizabilities for milrinone are equal to 7.7763 D and 3.90×10^{-30} esu for HF level and 7.1908 D and 6.76×10^{-30} esu for B3LYP level. Urea is one of the prototypical molecules used in the

Table 4 — Dipole moment μ, polarizability <α>, the anisotropic of the polarizability <Δα> and the mean first-order hyperpolarizability values obtained using HF and B3LYP level with 6-31G(d,p) methods for milrinone

	HF/6-31G(d,p)	B3LYP/6-31G(d,p)
μ (D)	7.7763	7.1908
<α> (a.u.)	132.53	141.83
<α>×10^{-24} (esu)	19.64	21.02
<Δα> (a.u.)	107.87	122.91
β (a.u.)	450.90	782.54
$\beta_{tot}\times10^{-30}$ (esu)	3.90	6.76
β_{tot}/β_{urea}	20	35

study of the NLO properties of molecular systems. Therefore it was used frequently as a threshold value for comparative purposes. Theoretically, dipole moments of milrinone are approximately both 2 times greater than urea and the mean first-order hyperpolarizabilities calculated at HF and B3LYP levels with 6-31G(d,p) basis set are 20 and 35 times magnitude of urea (the μ and β values of urea are 3.2877 D and 0.1947×10^{-30} esu), respectively. We conclude that the title compound is attractive objects for future studies of nonlinear optical (NLO) properties.

5 Conclusions

The structural, conformational, electronic and vibrational investigations along with NLO analysis of the milrinone were determined and analyzed using HF/6-31G(d,p) and DFT/6-31G(d,p) levels of theory. On the basis of the agreement between the calculated and observed results, assignments of fundamental vibrational modes of the title compound were examined based on the results of the PED output obtained from normal coordinate analysis. After scaling factors for 0.8991 (HF) and 0.9614 (B3LYP) are used, the calculated wavenumbers show good agreement with observed FTIR and FT-Raman spectra. Nonlinear optical property of the studied compound was investigated by the determination of the ground state dipole moment, the mean polarizability, the anisotropy of the polarizability and the mean first-order hyperpolarizability using the HF and B3LYP methods. So, it is demonstrated that the investigated compound can be used as a NLO material. The relatively small energy gap between the HOMO and LUMO energies proves that the charge transfer occur in milrinone. Additionally, the χ parameter was obtained from HOMO–LUMO energies, and the low χ values also indicate the presence of the charge transfer.

Acknowledgement

The author would like to thank Kocaeli University Research Fund for its financial support (Grant No. 2015/94).

References

1 Mišić-Vuković M, Mijin D, Radojković-Veličković M, Valentić N & Krstić V, *J Serb Chem Soc*, 63 (1998) 585.
2 Litvinov V P, Krivokolysko D & D Dayachenko V, *Chem Heterocycl Compd,* 35 (1999) 509.
3 Rigby J H, *Synlett*, 1 (2000).
4 Pastelin G, Mendez R, Kabela E & Farah A, *Life Sci***,** 33 (1983) 1787.
5 Presti E L, Boggia R, Feltrin A, Menozzi G, Dorigo P & Mosti L, *Farmaco*, 54 (1999) 465.
6 Dorigo P, Fraccarolo D, Gaion R M, Santostasi G, Borea P A, Floreani M, Mosti L & Maragno I, *Gen Pharm*, 28 (1997) 781.
7 Altomare C, Cellamare S, Summo L, Fossa P, Mosti L & Carotti A, *Bioorg Med Chem*, 8 (2000) 909.
8 Lo Presti E, Boggia R, Feltrin A, Menozzi G, Dorigo P & Mosti L, *Il Farmaco*, 54 (1999) 465.
9 Cody V, *Acta Cryst Sect C*, 43 (1987) 1325.
10 Frisch M J, *Gaussian 09, revision A 1*, *Gaussian Inc,* (Wallingford, CT), 2009.
11 Dennington R, Keith T & Millam J, *Gauss view, version 5.0.9*, (Semichem Inc, Shawnee Mission KS), 2009.
12 Becke A D, *J Chem Phys*, 98 (1993) 5648.
13 Lee C, Yang W & Parr R G, *Phys Rev B*, 37 (1988) 785.
14 Pople J A, Scott A P, Wong M W & Radom L, *Isr J Chem*, 33 (1993) 345.
15 Scott A P & Radom L, *J Phys Chem*, 100 (1996) 16502.
16 Jamroz M H, *Vibrational energy distribution analysis,* (VEDA 4, Warsaw, Poland), 2004.
17 Koopmans T C, *Phys A*, 1 (1933) 104.
18 Senet P, *Chem Phys Lett*, 275 (1997) 527.
19 Pauling L, *The nature of the chemical bond*, (Cornell University Press, Ithaca, New York), 1960.
20 Buckingham A D, *Adv Chem Phys*, 12 (1967) 107.
21 Mclean A D & Yoshimine M, *J Chem Phys*, 47 (1967) 1927.
22 Lin C & Wu K, *Chem Phys Lett*, 321 (2000) 83.
23 Abraham J P, Sajan D, Hubert I J & Jayakumar V S, *Spectrochim Acta Part A***,** 71 (2008) 355.
24 Karamanis P, Pouchan C & Maroulis G, *Phys Rev A*, 77 (2008) 013201.
25 Sağdınç S G & Eşme A, *Spectrochim Acta Part A***,** 75 (2010) 1370.
26 Sekar M, Velmurugan R, Chandramohan A, Rameshb P & Ponnuswamy M N, *Acta Cryst E*, 67 (2011) 3270.
27 Sert Y, Çırak, Ç & Ucun F, *Spectrochim Acta Part A*, 107 (2013) 248.
28 Arman H D, Poplaukhin P & Tiekink E R T, *Acta Cryst E*, 65 (2009) 3187.
29 Huang W & Qian H, *Dyes Pigm*, 77 (2008) 446.
30 Aquel R & Verma P K, *Indian J Pure Appl Phys*, 20 (1982) 665.
31 Colthup N B, Daly I H & Wiberley S E, *Introduction to infrared and raman spectroscopy*, 3rd Edn, (Academic Press, New York), 1990.
32 Socrates G, *Infrared and raman characteristic group frequencies*, 3nd Edn, (Wiley, New York), 1981.
33 Silverstein M, Clayton Basseler G & Moril C, *Spectro metric identification of organic compounds*, 2nd Edn, (Wiley, New York), 1981.
34 Alpert N L, Keiser W E & Szymanski H A, *Theory and practice of infrared spectroscopy*, 2nd Edn, (Plenum Press, New York), 1970.
35 Günay N, Tamer O, Kuzalic D, Avci D & Atalay Y, *Acta Phys Pol A*, 127 (2015) 701.
36 Sangeetha C C, Madivanane R & Pouchaname V, *Arch Phys Res*, 4 (3) (2013) 67.
37 Elamurugu Porchelvi E & Muthu S, *Spectrochim Acta Part A*, 134 (2015) 453.
38 Arivazhagan M & Senthilkumar J, *Spectrochim Acta Part A*, 137 (2015) 490.
39 Varsanyi G, *Assignments for vibrational spectra of seven hundred benzene derivatives*, 2nd Edn, (Wiley, New York), 1974.

40 Muthu S & Maheswari J U, *Spectrochim Acta Part A*, 92 (2012) 154.
41 Tanak H, Ağar A A & Buyukgungor O, *Spectrochim Acta Part A*, 87 (2012) 15.
42 Wang Y, Saebo S & Pittman C U, *J Mol Struct*, 281 (1993) 91.
43 Fleming J, *Frontier orbitals and organic chemical reactions*, (Wiley, London), 1976.
44 Eşme A & Sağdınç S G, *J Mol Struct*, 1048 (2013) 185.
45 Politzer P & Murray J S, *Theoretical biochemistry and molecular biophysics: A comprehensive survey*, 2nd Edn, (Adenine Press, New York), 1991.
46 Politzer P & Murray J, *Theor Chem Acc*, 108 (2002) 134.
47 Scrocco E & Tomasi J, *Top Curr Chem*, 42 (1973) 95.
48 Luque F J, Lopez J M & Orozco M, *Theor Chem Acc*, 103 (2000) 343.
49 Ditchfield R, *J Chem Phys*, 56, (1972) 5688.
50 Wolinski K, Hinton J F & Pulay P, *J Am Chem Soc*, 112 (1990) 8251.
51 Prasad O, Sinha L, Misra N, Narayan V, Kumar N & Pathak J, *J Mol Struct*, 940 (2010) 82.
52 Cheeseman J R, Trucks G W, Keith T A & Frisch M J, *J Chem Phys*, 104 (1996) 5497.